Conference materials
UDC 535.215.6
DOI: https://doi.org/10.18721/JPM.161.220

Interference pattern analysis approach for sensory applications

I.V. Kuznetsov[1]✉, A.S. Perin[1]

[1] Tomsk State University of Control Systems and Radioelectronics, Tomsk, Russia

✉ kuznetsov.i.159@e.tusur.ru

Abstract. This paper presents the results of a new approach to the analysis of interference patterns in the modulator output waveguide in a Mach-Zehnder interferometer configuration based on lithium niobate thin films. Interference patterns that occur in the output waveguide have been demonstrated. An approach of analysis of the patterns has been described. The method allows us to obtain information about the value of voltage applied to the arm of the interferometer and to double upper limit of measuring electric field strength using MZI based electro-optic modulator.

Keywords: Mach-Zehnder interferometer, interference pattern, electro-optic sensor

Funding: The research was carried out within the state assignment of Ministry of Science and Higher Education of the Russian Federation (No. FEWM-2022-0004).

Citation: Kuznetsov I.V., Perin A.S., Interference pattern analysis approach for sensory applications, St. Petersburg State Polytechnical University Journal. Physics and Mathematics. 16 (1.2) 2023 133–138. DOI: https://doi.org/10.18721/JPM.161.220

Материалы конференции
УДК 535.215.6
DOI: https://doi.org/10.18721/JPM.161.220

Подход к анализу интерференционных картин для сенсорных приложений

И.В. Кузнецов[1]✉, А.С. Перин[1]

[1] Томский государственный университет систем управления и радиоэлектроники, г. Томск, Россия

✉ kuznetsov.i.159@e.tusur.ru

Аннотация. В данной работе представлен новый подход к анализу интерференционных картин в выходном волноводе интегрального интерферометра Маха-Цендера, сформированного из гребенчатых волноводов на основе тонкой пленки ниобата лития. Использование представленного подхода может двухкратно увеличить динамический диапазон электрооптических сенсоров электрического поля.

Ключевые слова: интерферометр Маха-Цендера, интерференционные картины, электрооптический сенсор

Финансирование: Работа выполнена в рамках государственного задания Министерства науки и высшего образования Российской Федерации (№ FEWM0004-2022-).

Ссылка при цитировании: Кузнецов И.В., Перин А.С. Подход к анализу интерференционных картин для сенсорных приложений // Научно-технические ведомости СПбГПУ. Физико-математические науки. 2023. Т. 16. № 1.2. С. 133–138. DOI: https://doi.org/10.18721/JPM.161.220

Introduction

Currently, integrated optoelectronic devices are widely used. They are characterized by compact size, high noise immunity and wide bandwidth due to the use of light as a carrier wave.

Due to its low cost and wide transparency window, lithium niobate remains one of the main materials in optoelectronics. It is possible to manufacture integrated optical circuits by the method of titanium diffusion into a lithium niobate crystal [1]. The advantage of this method is the possibility of providing a single-mode waveguide due to the small physical dimensions of the resulting waveguides and the small difference between the refractive indices of the waveguide core and its cladding, which can be important for use in telecommunication systems. The disadvantage of this method is the need to use centimeter-sized lithium niobate crystals, which does not meet modern trends in miniaturization of devices. Also the use of the titanium diffusion method is associated with the risk of cracking in the lithium niobate crystal, since the technology involves heating the crystal to temperatures above 1000 °C.

The compact dimensions of the optoelectronic device can be achieved by using thin films of lithium niobate. The method of applying thin films of lithium niobate by Radio frequency magnetron sputtering (RFMS) is promising. RFMS makes it possible to deposit thin films of lithium niobate up to 100 nm thick on semiconductor substrates at a temperature of 500 °C [2]. The ability to deposit a thin film on a semiconductor substrate at such temperatures makes it possible to implement potentially a device that has an optical and electronic integrated circuit on the same chip. The disadvantage of RFMS is that the deposited thin films have a polycrystalline structure. Such a structure can cause high optical losses during light propagation through the film. Controlling of the crystallites orientations of the RFMS thin film is also a problem.

Thin films made using the Lithium Niobate on Insulator (LNOI) method are more widespread. LNOI also allows one to deposit a thin film with a thickness of less than one micron. It is possible to choose the orientation of the film. The disadvantage of LNOI is the technological need to heat the film sample to temperatures above 900 °C, which can cause cracking and destruction of a thin film [3].

The Mach-Zehnder interferometer (MZI) is one of the basic components of integrated optoelectronics. It is possible to create electric field sensors, electro-optical switches, optical radiation intensity modulators and other optoelectronic devices based on MZI [1, 4–9].

One of the promising applications of the MZI is the electric field sensor systems. Various configurations of MZI based electric field sensors are known [1, 10]. Their upper limits of the range of measuring electric field strength are different depending on electrodes length. However, the presented sensors use the same method of analyzing output optical signal: calculating modulator transmission coefficient. This method limits upper range of the measuring electric field strength to the strength corresponding to the half-wave voltage of the modulator.

Hence, the purpose of this work is to study a new approach of analyzing output optic signal of an electro-optical modulator in the configuration of a Mach-Zehnder interferometer based on ridge waveguides made of a thin film of lithium niobate, using FFT BPM.

To perform the study, a simulation of the operation of an electro-optical intensity modulator based on MZI based on FFT BPM was carried [11–14].

FFT-BPM

The beam propagation method (BPM) is a method for approximating the solution of the Helmholtz equation. As part of this work, a program has been implemented that realizes an FFT based on the fast Fourier transform (FFT) [11, 13].

BPM considers the propagation of an electromagnetic field on a plane as a function of two coordinates u(x, z), where x is a coordinate of a point along the axis of the transverse axis of light propagation, z is coordinate along the axis of light propagation. If the value of the field at the point (x, z_0), is known then the value of the field at the point (x, $z_0+\Delta z$) can be found as:

$$u(x, z_0 + \Delta z) = \Psi(x, z_0 + \Delta z)\exp(i\Gamma), \quad (1)$$

where Ψ is the wave function, Γ is phase factor, calculated as:

$$\Gamma = \frac{k^2 - \beta^2}{2\beta} dz,$$

where k is the wavenumber, β is the propagation constant. We apply the discrete Fourier transform to the wave function and get:

$$\Psi_n(x_i, z) = \frac{1}{N} \sum_{n=-N/2}^{N/2} \Psi_n(z) \exp(ik_n x_i), \quad (2)$$

where $k_n = 2\pi n / N\Delta x$ and N is the number of samples, obtaining

$$\Psi_n(x_i, z) = \frac{1}{N} \sum_{n=-N/2}^{N/2} \Psi_n(z) \exp(ik_n x_i). \quad (3)$$

Hence, the problem of calculating the propagation of light is solved by the following algorithm:

1. Perform the discrete Fourier transform to the wave function $\Psi(x,z_0)$, to get $\Psi_n(z_0)$.
2. Calculate $\Psi_n(x, z_0+\Delta z)$ from (1.1).
3. Perform the inverse discrete Fourier transform to the $\Psi_n(z_0 + \Delta z)$, to get $\Psi(x, z_0 + \Delta z)$.
4. If the coordinate $(z_0 + \Delta z)$ does not correspond to the point at which the calculation should stop, then, then $z_0 = z_0 + \Delta z$ and return to the point 1.

MZI Configuration

In this paper, we will consider a modulator based on a Mach–Zehnder interferometer, made of ridge waveguides made of Z-cut lithium niobate thin film. The geometric parameters of the interferometer are shown in Fig. 1.

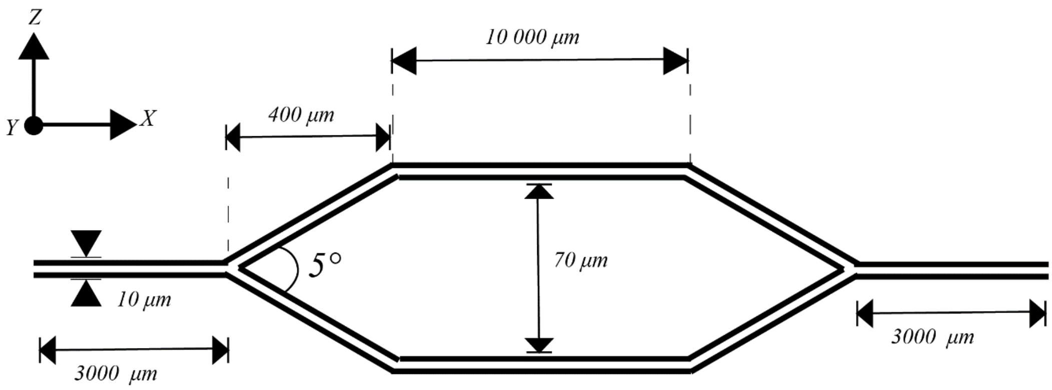

Fig. 1. MZI configuration and orientation of the thin film

Half wave voltage of a MZI modulator is determined by:

$$U_{\frac{\lambda}{2}} = \frac{\lambda d}{n_e^3 r_{33} L}, \quad (4)$$

where λ = 633 nm is the wavelength of the light, d = 10 μm is the width of the waveguides, n_e = 2.2139 is the extraordinary refractive index of the lithium niobate thin film, L is length of the electrodes. Thus, half-wave voltage of represented modulator is 1.93 V.

This simulation was performed using 2D model. Some parameters including waveguide highness and film thickness were not taken into account. However, we note that modern integrated ridge waveguides have highness in range of hundreds of nanometers [15, 16].

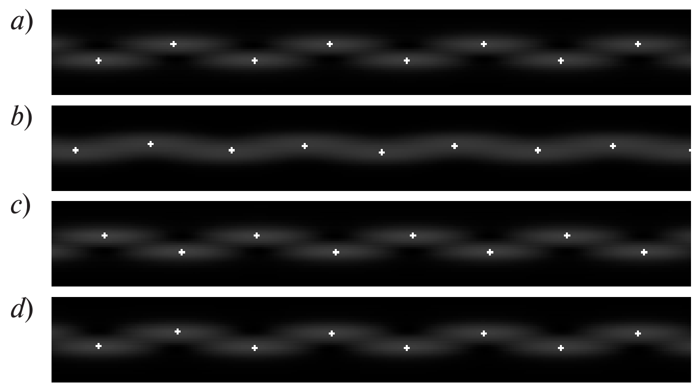

Fig. 2. Interference patterns at various applied voltages:
0.5 V (*a*); 1.5 V (*b*); 2.43 V (*c*); 4.36 V (*d*)

Simulation parameters and results

The wavelength of light was taken to be 633 nanometers, the light was extraordinary polarized, the refractive index of the core of the waveguides was 2.2139, the refractive index of the environment was taken to be 1, the electro-optical coefficient r_{33} was taken to be 30.8 pm·V^{-1} [17-19]. The geometric parameters of the interferometer are shown in Fig. 1.

As a result of simulation, interference was observed in the output waveguide. Images of parts of the interference patterns (top view) at various values of the applied voltage are shown in Fig. 2, where the white dots indicate the interference maxima.

As can be seen from Fig. 2, at applied voltages of 0.5 V and 4.36 V, the distribution of interference maxima has an identical character. Also, in the interference patterns corresponding to applied voltages of 0.5 V and 2.43 V, there is a change in places of the maxima and minima of the interference relative to each other. Thus, patterns corresponding to voltages differing by 1.93 V are in antiphase, and patterns corresponding to voltages differing by 3.86 V are in the same phase. This confirms the above calculation of the half-wave voltage for the given configuration of the interferometer.

Also the presence of this cycle is confirmed by the dependence of the distance between the maxima of the interference pattern on the applied voltage, presented graphically in Fig. 3.

As can be seen from Fig. 3, the same distance between the interference maxima is repeated with a frequency of 3.86 V. This also confirms that the interference patterns spaced 3.86 V apart are in the same phase, and the half-wave voltage is 1.93 V.

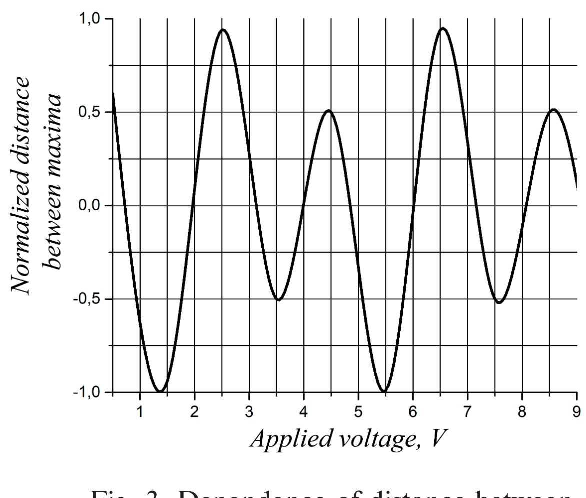

Fig. 3. Dependence of distance between interference maxima on applied voltage

To analyze such interference patterns, in order to extract information about the magnitude of the applied electric field, it is possible to use detectors that determine the distances between adjacent maxima and their position relative to each other. This approach makes it possible to double the measurement range of the electric field strength compared to the measurement of the modulator transmission coefficient.

Conclusion

Thus, the FFT BPM method was used to study a new approach to the analysis of interference patterns of output waveguide of an electro-optical modulator based on a Mach–Zehnder interferometer made based on ridge waveguides made of thin films of lithium niobate. The simulation of the modulator with a given configuration was carried out. According to the results of the simulation, the considered configuration has a half-wave voltage equal to 1.93 V. Interference patterns arising in the output waveguide of the modulator were presented and considered, and an approach for their analysis was also proposed, based on determining the distance between the interference maxima. Determined that the proposed approach allows to double upper limit of measuring electric field strength in case of MZI-based electric field sensor.

REFERENCES

1. **Jung H.,** An integrated photonic electric-field sensor utilizing a 1×2 YBB Mach–Zehnder interferometric modulator with a titanium-diffused lithium niobate waveguide and a dipole patch antenna, Crystals. 9 (9) (2019) 459.
2. **Dybov V.A., Serikov D.V., Ryzhkova G.S.,** Growth and substructure of lithium niobate films, Condensed media and interfaces. 21 (1) (2019) 51–59.
3. **Soham S., Siew S. Y., Deng J., Aaron D., Mankei T.,** Fabrication and characterization of optical devices on lithium niobate on insulator chips, Procedia Engineering. (140) (2016) 183–186.
4. **Xiaobo Xie, Khurgin J., Kang J., Chow F.,** Linearized Mach-Zehnder intensity modulator, IEEE Photonics Technology Letters. 15 (4) (2003) 531–533.
5. **Nikolajsen T., Leosson K., Bozhevolnyi S.I.,** Surface plasmon polariton based modulators and switches operating at telecom wavelengths, Applied Physics Letters. 85 (24) (2004) 5833–5835.
6. **Petraru A., Schubert J., Schmid M., Trithaveesak O., Buchal Ch.,** Integrated optical Mach Zehnder modulator based on polycrystalline BaTiO 3, Optics letters. 28 (24) (2003) 2527–2529.
7. **Ran H., Wei D., Hongsheng C., Xiaofeng J., Longzhi Y., Erping L.,** Ultra-compact optical modulator by graphene induced electro-refraction effect, Applied Physics Letters. 103 (6) (2013) 061116.
8. **Singh G., Yadav R. P., Janyani V.,** Ti indiffused lithium niobate (Ti: LiNbO3) Mach-Zehnder interferometer all optical switches: a review, New Advanced Technologies. (2010).
9. **Wang C., Zhang M., Chen X., Bertrand M., Shams-Ansari A., Sethumadhavan Ch, Winzer P., Lončar M.,** Integrated lithium niobate electro-optic modulators operating at CMOS-compatible voltages, Nature. 562 (7725) (2018) 101–104.
10. **Zhang J., Yang L., Li Y.,** Non-invasive measurement of intensive power-frequency electric field using a LiNbO3-integrated optical waveguide sensor, IET Science, Measurement & Technology. 15 (1) (2021)101-108.
11. **Samra A., Yousif B.B.,** Beam Propagation Method Based on Fast Fourier Transform and Finite Difference Schemes and its Application to Optical Diffraction Grating. (Dept. E), MEJ. Mansoura Engineering Journal.31 (1) (2020) P. 67–81.
12. **Devi P., Maddila R.K.,** Modeling of lithium niobate based Mach-Zehnder modulator for visible light communication system with BER analysis, Optical and Quantum Electronics. 53 (6) (2021) 1-15.
13. **Singh G., Janyani V., Yadav R.P.,** Modeling of a 2× 2 electro-optic Mach-Zehnder Interferometer optical switch with s-bend arms, Photonics letters of Poland. 3 (3) (2011) 119–121.
14. **Van Roey J., Van der Donk J., Lagasse P.E.,** Beam-propagation method: analysis and assessment, Josa. 71 (7) (1981) 803-810.
15. **Poberaj G. Hu. H., Sohler W.,Guenter P.,** Lithium niobate on insulator (LNOI) for microphotonic devices, Laser & photonics reviews. 6 (4) (2012) 488–503.
16. **Wang Y., Chen Z., Hu H.,** Analysis of waveguides on lithium niobate thin films, Crystals. 8 (5) (2018) 191.

17. **Smith D.S., Riccius H.D., Edwin R.P.,** Refractive indices of lithium niobate, Optics communications. 17 (3) (1976) 332–335.

18. **Turner E.H.,** High-frequency electro-optic coefficients of lithium niobate, Applied Physics Letters. 8 (11) (1966) 303-304.

19. **Han H., Cai L., Hu H.,** Optical and structural properties of single-crystal lithium niobate thin film, Optical Materials. 42 (2015) 47-51.

THE AUTHORS

KUZNETSOV Igor V.
kuznetsov.i.159@e.tusur.ru
ORCID: 0000-0002-4226-0500

PERIN Anton S.
anton.s.perin@tusur.ru
ORCID: 0000-0002-9597-3088

Received 18.10.2022. Approved after reviewing 14.11.2022. Accepted 15.11.2022.